Dissociation of molecular chlorine in a Coulomb explosion: Potential curves, bound states, and deviation from Coulombic behavior for Cl_2^{n+} (n=2,3,4,6,8,10)

Wright, J. S.; Dilabio, G. A.; Matusek, D. R.; Corkum, P. B.; Ivanov, M. Yu.; Ellert, Ch.; Buenker, R. J.; Alekseyev, A. B.; Hirsch, G.

National Research Council Canada   Conseil national de recherches Canada

Canada

Dissociation of molecular chlorine in a Coulomb explosion: Potential curves, bound states, and deviation from Coulombic behavior for Cl_2^{n+} ($n=2,3,4,6,8,10$)

J. S. Wright,* G. A. DiLabio, and D. R. Matusek

Department of Chemistry, Carleton University, 1125 Colonel By Drive, Ottawa, Canada K1S 5B6

P. B. Corkum, M. Yu. Ivanov, and Ch. Ellert

Steacie Institute for Molecular Sciences, National Research Council of Canada, Ottawa, Canada K1A 0R6

R. J. Buenker, A. B. Alekseyev, and G. Hirsch

Bergische Universität-Gesamthochschule Wuppertal, Fachbereich 9, Theoretische Chemie, Gausssstrasse 20, D-42097 Wuppertal, Germany

Highly charged molecular ions are generated in Coulomb explosion experiments involving multielectron dissociative ionization, but little is known about the precise mechanisms involved in their formation. To help improve the understanding of such experiments, potential energy curves are calculated in this paper for diatomic chlorine (Cl_2) and its ions Cl_2^{n+}, where $n=1,2,3,4,6,8,10$. Bound vibrational states are obtained in three low-lying electronic states for Cl_2^{2+} and one state for Cl_2^{3+}. Vertical excitation energies are given for stepwise excitations up to Cl_2^{10+}. For all the ions examined there is a significant energy defect (Δ) from the corresponding Coulomb potential, in one case reaching magnitudes of over 20 eV. We analyze the origin of these energy defects in terms of residual chemical bonding, and discuss the contribution of strongly bonding configurations at short internuclear distance. Finally, we present a simple physical model which describes the qualitative behavior of $\Delta(R,Q)$. [S1050-2947(99)01606-6]

PACS number(s): 42.50.Hz, 33.80.Gj, 31.15.−p, 33.40.+f

I. INTRODUCTION

Coulomb explosion imaging, first introduced in 1979 [1], provides a general approach to measuring the geometry of small molecules. The image is obtained by (i) removing many electrons from a molecule with the nuclei confined by their own inertia and (ii) collecting all fragment atomic ions, and measuring their charge and velocity vector [2]. The ability to deduce a range of possible initial molecular geometries requires knowledge of the potential surface of the highly charged molecular ion. The term Coulomb explosion imaging refers to the assumption that the internuclear potential energy surface can be approximated by the Coulomb interaction between the fragment atomic ions.

The assumption that Coulomb repulsion describes the internuclear force in highly charged molecules is central to any of the approaches to Coulomb explosion imaging. We test the validity of this assumption for Cl_2^{n+}. We show that there are very large deviations from the Coulomb potential even when most of the bonding electrons are removed. Our calculations set a practical limit on the measurement accuracy that Coulomb explosion imaging can ultimately achieve.

In Coulomb explosion imaging experiments, electron removal is usually accomplished by passing a high kinetic energy molecular ion through a sub-100 Å gold foil. During the 0.1−1-fs transit time through the foil the weakly bound electrons are stripped. Recently, however, another approach has

been introduced: Very high power femtosecond laser pulses can remove many electrons from a molecule within the duration of the laser pulse, which can be short as 5 fs [3].

Because of the simplicity of laser techniques, Coulomb explosion imaging will be transformed by laser methods. Furthermore, optical techniques allow molecular dynamics to be initiated with a pump pulse and observed in real time with a probe pulse. A Coulomb explosion experiment of this kind has recently been done [4].

Ideally, optical Coulomb explosion imaging will use laser pulses so short that the ion motion will occur on a field-free potential surface. However, even with the shortest optical pulses currently available, there is time for some motion of the light elements on the strongly repulsive potential surfaces and the presence of a strong laser field will severely distort the potential energy surface of the ion. With the potential energy surfaces established in this paper, modeling the changes caused by dissociation on laser-distorted potential energy surfaces will be the subject of a following paper.

Already there is a wealth of experimental data on Coulomb explosions initiated with moderately short pulses. One notable observation from these experiments is that the kinetic energy release is significantly less than that expected from purely Coulombic behavior arising from vertical excitation at the equilibrium internuclear distance of the uncharged diatomic, and is surprisingly insensitive to the pulse duration. Deviation from Coulomb behavior caused by residual bonding is not a surprise [5–9] and has been studied by many authors. Ours is the first systematic study, however, up to very high charge states. We show that even for Cl_2^{10+} the deviation from the Coulomb potential can be as large as 13 eV at the equilibrium distance of the neutral molecule.

*Author to whom correspondence should be addressed. Electronic address: jim_wright@carleton.ca

Since molecules have never been exposed to such intensities before, it would not be surprising if new phenomena emerged. Laser-induced bonding of highly charged molecules [10], dynamic screening [11], and a high sensitivity of the ionization rate to the internuclear separation [12] are three examples of phenomena that have been proposed to explain the surprisingly large energy defect. There is now a need for a systematic theoretical work to discriminate between possible models. By showing that large deviations from a Coulomb potential are characteristic of high-charged states of the halogen molecules, we quantify one important, but often underestimated, reason for this ''energy defect.'' A forthcoming paper will consider the polarizability of the even-charged ions, the effect of the laser field on their potential energy curves (multielectron laser-induced bonding) and attempt a complete modeling for the Coulomb explosion experiment for Cl_2^{n+}.

II. METHOD OF CALCULATION

Diatomic chlorine Cl_2 and its monocation Cl_2^+ have been well studied experimentally [13–15]. Among the most important spectroscopic parameters are the dissociation energy D_0, the equilibrium internuclear distance R_e, the harmonic vibration frequency ω_e and the vertical ionization potential IP. Theoretically, these parameters can be obtained by calculating the total energy at selected R and then fitting the data to an appropriate functional form, e.g., a 3-parameter Morse function of the form $V = D_e[1 - \exp(-\beta x)]^2 - D_e$, where $x = (R - R_e)$. These forms are appropriate to the neutral Cl_2 and the monocation Cl_2^+. In the present work we wish to fit curves of more complex shape, including metastable minima, so the data were interpolated using natural cubic splines. These potential curves were then used as input to a Numerov-Cooley procedure [16] for solving the Schrödinger equation to obtain the vibration-rotation energy levels $E_{v,J}$. For Cl_2 and Cl_2^+ the resulting energy levels were fit to a standard spectroscopic expression of the form $E_{v,J} = (v + \frac{1}{2})\omega_e - (v + \frac{1}{2})^2\omega_e x_e + BJ(J+1) - \alpha(v + \frac{1}{2})(J+1)$, where $\omega_e x_e$ is the anharmonicity constant and B and α are rotational and rotation-vibration constants, respectively. The difference between the zero-point energy $E_{0,0}$ and the dissociation limit is the dissociation energy D_0. In the case of Cl_2 and Cl_2^+, D_0 is (to a good approximation) related to the well depth D_e by $D_e = D_0 + \frac{1}{2}\omega_e - \frac{1}{4}\omega_e x_e$.

In calculating the entire potential curve, and especially for the higher-charged ions, traditional quantum-chemistry perturbation techniques [17] such as Moller-Plesset second-order perturbation theory (MP2) and fourth-order (MP4) are unreliable, since they are based on single-determinant wave functions. Instead, multireference configuration interaction (MR-CI) methods which provide suitable configuration mixing en route to dissociation are preferred. A very thorough MRD-CI study of the electronically excited and first-ionized states of the chlorine molecule was given by Peyerimhoff and Buenker in 1981 [18], where the notation implies single and double excitations from a chosen set of reference configurations. These authors used a basis set consisting of $5s5p2d$ contracted functions on Cl derived from the primitive Gaussian basis of McLean and Chandler [19]. They also added (s,p) bond functions to describe polarization effects

TABLE I. Species, electronic state, number of reference configurations, dominant reference configuration and formal bond order (B.O.) for the ions Cl_2^{n+}.

Species	State	No. Ref.	Dominant Ref.	B.O.
Cl_2	$^1\Sigma_g^+$	4	$(2\pi_u)^4(2\pi_g)^4$	1.0
Cl_2^+	$^2\Pi_g$	13	$(2\pi_u)^4(2\pi_g)^3$	1.5
Cl_2^{2+}	$^3\Sigma_g^-$	6	$(2\pi_u)^4(2\pi_g)^2$	2.0
Cl_2^{2+}	$^1\Delta_g$	28	$(2\pi_u)^4(2\pi_g)^2$	2.0
Cl_2^{2+}	$^1\Sigma_g^+$	28	$(2\pi_u)^4(2\pi_g)^2$	2.0
Cl_2^{3+}	$^2\Pi_g$	12	$(2\pi_u)^4(2\pi_g)^1$	2.5
Cl_2^{3+}	$^2\Sigma_u^+$	14	$(2\pi_u)^4(2\pi_g)^1$	2.5
Cl_2^{4+}	$^1\Sigma_g^+$	14	$(2\pi_u)^4$	3.0
Cl_2^{6+}	$^3\Sigma_g^-$	8	$(2\pi_u)^2$	2.0
Cl_2^{6+}	$^1\Delta_g$	22	$(2\pi_u)^2$	2.0
Cl_2^{8+}	$^1\Sigma_g^+$	30	$(5\sigma_g)^2(2\pi_u)^0$	1.0
Cl_2^{8+}	$^3\Sigma_g^-$	9	$(5\sigma_g)^0(2\pi_u)^2$	1.0
Cl_2^{8+}	$^1\Delta_g$	30	$(5\sigma_g)^0(2\pi_u)^2$	1.0
Cl_2^{10+}	$^1\Sigma_g^+$	30	$(4\sigma_g)^2(4\sigma_u)^2$	0.0

and diffuse (s,p) Rydberg functions midway between the two nuclei to describe Rydberg series. In our calculations we expanded the basis of contracted functions to $10s7p2d$ on each Cl atom and included extra (s,p) functions with exponent 0.5 midway between the Cl atoms. Using 6-component d functions, our basis contains a total of 90 functions [20]. The MRD-CI program package of Buenker and co-workers [21,22] was used in this study.

Several features of the MRD-CI treatment are common to all the ions treated here. For neutral Cl_2, for example, SCF-MO's were generated from the ground-state configuration for Cl_2, corresponding to the MO occupation $[Ne]_2(4\sigma_g)^2(4\sigma_u)^2(5\sigma_g)^2(2\pi_u)^4(2\pi_g)^4$. Here $[Ne]_2$ is the closed-shell core containing 20 electrons. For all calculations, the 20 core electrons were frozen in the 10 lowest MO's, and the corresponding 10 highest-lying MO's were discarded, leaving $14 - n$ electrons (Cl_2^{n+}) to be correlated in the MRD-CI calculation involving 70 MO's. An energy selection threshold of 5 μhartree was chosen for the CI energy extrapolation in all calculations. Single- and double-excitations from the reference configurations, followed by a perturbation selection procedure led to selected CI spaces of dimension ca. 6000–16 000 spin and symmetry-adapted functions (SAF's). In general, reference configurations were included in the calculation whenever their (squared) contribution to the final CI eigenvector exceeded 0.002. This led to CI expansions which generally (for all ions) contained $\geq 90\%$ contribution (on a coefficient-squared basis) from the reference configurations over the whole range of internuclear distances. The root of the diagonalization was then extrapolated to zero selection threshold and corrected for quadruple excitations in the usual way with the multireference analog of the Langhoff-Davidson correction [23] to obtain the final total energy, which for simplicity we denote simply the ''CI energy, or E_{CI},'' from which the spectroscopic constants were derived. The grid of data values was taken in increments of 0.2 bohr from 2.0–4.2 bohr, with additional points at 4.5, 5.0, 6.0, 8.0, 10.0, and 20.0 bohr.

In order to present the characteristics of the CI treatment

TABLE II. Well depth D_e, internuclear distance R_e, and spectroscopic parameters $D_0, \omega_e, \omega_e x_e$ for Cl_2 $(X \, {}^1\Sigma_g^+)$ and Cl_2^+ $(X \, {}^2\Pi_g)$.

Quantity	Calc'd.	Ref. [18][a]	Expt.[b]
Cl_2:			
D_e (eV)	2.573	2.490	2.514[c]
R_e (bohr)	3.820	3.817	3.757
D_0 (eV)	2.539	2.455	2.479
ω_e (cm^{-1})	560	552	560
$\omega_e x_e$ (cm^{-1})	2.87		2.67
Cl_2^+:			
D_e (eV)	3.697	~3.40[d]	4.030
R_e (bohr)	3.642	3.628	3.574
D_0 (eV)	3.659	~3.36[c]	3.990
ω_e (cm^{-1})	620	620	646
$\omega_e x_e$ (cm^{-1})	2.65		3.02

[a]From theoretical calculation of Peyerimhoff and Buenker [18].
[b]Experimental data in Tables I and II from Ref. [13].
[c]Using $D_e = D_0 + \omega_e/2 - \omega_e x_e/4$.
[d]Estimated from Fig. 2 of Ref. [18].

in a compact form, Table I shows the (dominant) configuration, electronic state, number of reference configurations used for that state, and MO bond order. The starting MO's used to generate the CI states may sometimes vary from the dominant configuration, and the state may change its character along the potential curve; these effects are discussed in context. The same general approach and basis set was used for the calculation of all ions up to $+10$. The accuracy of the calculations may begin to degrade for the higher-charged states, however. This occurs for two reasons. First, the inner $2s^2 2p^6$ electrons are more strongly perturbed when the charge is very high, and it would be desirable to correlate them as well in the CI calculation (not done here). Second, as the number of $3p$ electrons decreases, the $3p$ orbital becomes more compact. This leads in turn to a stronger spin-orbit interaction. The latter is certainly present at both atomic and molecular levels, but the difference between them must also become larger. In other words, spin-orbit effects which were neglected in our treatment will become more important for $n = 6, 8, 10$. The Cl atom has a rather small spin-orbit interaction, however, and these effects will probably not influence any of our conclusions.

III. RESULTS

Cl_2 and Cl_2^+. For $Cl_2(X^1\Sigma_g^+)$ and $Cl_2^+(X^2\Pi_g)$ the SCF-MO's used to construct the CI space were generated from the Cl_2 ground-state configuration given in Table I, i.e., $\ldots (4\sigma_g)^2(4\sigma_u)^2(5\sigma_g)^2(2\pi_u)^4(2\pi_g)^4$. Since $(4\sigma_g, 5\sigma_g, 2\pi_u)$ are bonding MO's and $(4\sigma_u, 2\pi_g)$ are antibonding, and defining in the usual way the formal bond order (B.O.) as [number of electrons in bonding molecular orbitals − number of electrons in antibonding molecular orbitals]/2, the B.O. of Cl_2 is 1.0 and Cl_2^+ is 1.5, so a decrease in bond length and an increase in well depth is expected on ionization. Table II shows the spectroscopic parameters for Cl_2 and Cl_2^+ obtained from the MRD-CI calculation.

In Table II the result for D_e in Cl_2 is slightly above the

experimental value and not quite as close as the calculated value of Peyerimhoff and Buenker [18]. Note, however, that if spin-orbit interaction is included the value of D_e will become smaller, further improving the agreement with the experimental value. The anharmonicity parameter $\omega_e x_e$ is also in good agreement with experiment, showing that the potential curve is well described at large displacements from equilibrium. The equilibrium internuclear distance R_e is slightly long for both Cl_2 and Cl_2^+, but the change in R_e on ionization is negative, as expected, and almost perfectly calculated ($\Delta R_e = -0.094$ Å calculated vs -0.097 Å experimental). The dissociation energy D_0 in the ion Cl_2^+ is somewhat underestimated (3.66 vs 3.99 eV), but closer than the value we estimated from the calculated potential curve in Ref. [18]. The vertical ionization potential calculated from our two potential curves is 11.36 eV, which is close to the experimental value of 11.50 eV. For the situation where the potential curves are known experimentally, then, the MRD-CI approach and basis set used is giving a generally satisfactory description.

Cl_2^{2+}. There have been several reports in the literature on the experimental observation of the dication Cl_2^{2+}. Measurement of the energy release of the dication in a double mass spectrometer by Beynon *et al.* [24] led to the conclusion that a metastable state was formed. A combined experimental/theoretical study by Fournier *et al.* [25] using double charge transfer and MRD-CI techniques similar to those in the present paper led to identification of several bound states. Most recently McConkey *et al.* [26] have observed vibrational transitions in the ground state and may have seen vibrational transitions in the first excited state as well.

The analogous member of the halogen family F_2^{2+} has been shown in theoretical work by Senekowitch and O'Neil [27] to have a local minimum bound by an effective barrier height $D_{eff} = 0.40$ eV. These authors argued that the local (metastable) minimum can be explained in terms of the mixing of a normal bound Morse potential similar to the isoelectronic molecule dioxygen, plus the Coulomb repulsion arising from the lower dissociation limit $F^+ + F^+$ (chemical bonding + Coulomb repulsion model) [28], and obtained good fits to the calculated data using this model. Another view of the cause of the metastable minimum in diatomic dications [29–31] is that it arises from an avoided crossing between the repulsive potential curve correlating with $F^+ + F^+$ and the attractive potential curve correlating with $F + F^{2+}$, the latter asymptote lying ca. 18 eV above the former. The origin of the attraction for the asymmetric channel is the charge-induced polarization of the F atom by the F^{2+} ion. The same considerations apply to Cl_2^{2+}, where the channel separation is only 11 eV and hence the interaction is stronger, possibly leading to a more deeply bound metastable minimum.

The electron configuration of the dication (Table I) has bond order $= 2.0$. The electron configuration π_g^2 leads to three electronic states ${}^3\Sigma_g^-$, ${}^1\Delta_g$ and ${}^1\Sigma_g^+$. In addition, the strongly bonding excited configuration $\ldots (5\sigma_g)^2(2\pi_u)^4(5\sigma_u)^2$ may contribute to the creation of a local minimum in the ${}^1\Sigma_g^+$ state. For this reason and because these three states were found to be metastable by Fournier
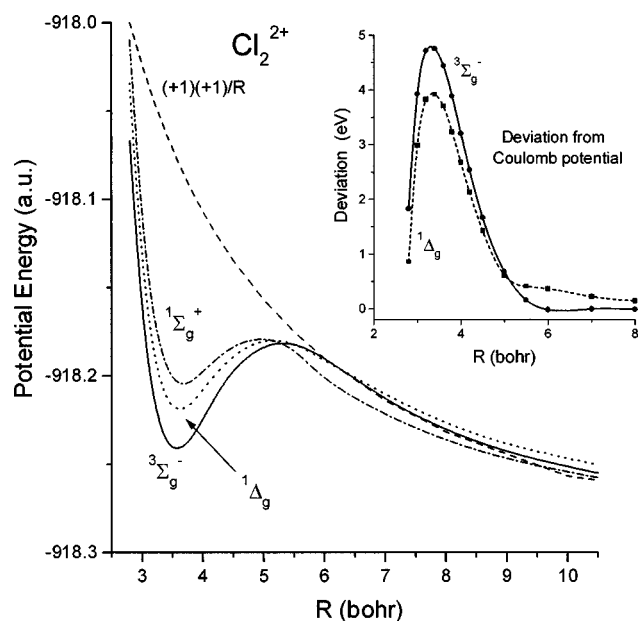
FIG. 1. Potential curves for Cl_2^{2+}, showing the three electronic states derived from the MO configuration $\ldots(\pi_g)^2$. Dashed line: Coulomb potential. Inset: Deviation from Coulomb potential for the two lowest-lying states of Cl_2^{2+}.

et al. [25], potential curves were calculated for both the ground electronic state $^3\Sigma_g^-$ and the low-lying electronic excited states $^1\Delta_g$ and $^1\Sigma_g^+$.

SCF-MO's for both states were generated from the triplet ground-state configuration of Cl_2^{2+}. Figure 1 shows the threelow-lying electronic states obtained along with the Coulomb potential corresponding to $(+1)(+1)/R$, i.e., the channel corresponding to $Cl^+ + Cl^+$ treated as point charges. It is clear from Fig. 1 that beyond 10 bohr, the Coulomb potential approaches an exact representation of the interaction potential. Properties derived for the three electronic states by this procedure are shown in Table III. This table includes R_{max}, the internuclear distance at the maximum in the potential curve, and D_{eff}, the energy difference between the (metastable) minimum at R_e and the potential energy at R_{max}.

The Cl_2^{2+} dication is isoelectronic with diatomic sulfur, and the two molecules have some common features, which are also shared by diatomic oxygen. The ground state is $^3\Sigma_g^-$, which lies nearly vertically below the first excited

TABLE III. Properties of the potential curves for Cl_2^{2+} in the three lowest-lying electronic states.

Property	$^3\Sigma_g^-$	$^1\Delta_g$	$^1\Sigma_g^+$
R_e (bohr)	3.568	3.624	3.676
R_{max} (bohr)	5.304	5.147	4.971
D_{eff} (eV)	1.701	1.154	0.784
ZPE (eV)	0.039	0.036	0.035
ω_{01} $(cm^{-1})^a$	626	585	569
No. v levels	27	20	13
T_e (eV)	0.00	0.611	1.003

$^a\omega_{01}$ is the energy spacing (in cm^{-1}) between the first two bound vibrational states.

state ($^1\Delta_g$), which in turn lies nearly vertically below the next excited state ($^1\Sigma_g^+$). The term energies T_e (Table III) also show a relative spacing almost identical to O_2, which has $T_e = (0.000, 0.982, 1.636$ eV) or $(0.0:0.60:1.00)$ [13].

Each of the three electronic states in Cl_2^{2+} is metastable and will support a manifold of bound vibrational states. As shown in Table III, the effective classical barrier heights (i.e., without considering zero-point energy) are 1.70, 1.15, and 0.78 eV, deep enough to support 27, 20, and 13 bound levels, respectively. Unlike O_2 and other neutral diatomics, the potential is very harmonic for the first few vibrational states: in fact, there is a slight *increase* in the transition frequency on excitation, i.e., $(626, 630, 634, 632$ $cm^{-1})$ in the $^3\Sigma_g^-$ state for 0-1, 1-2, 2-3, and 3-4, respectively.

For comparison, consider the theoretical results of Fournier *et al.* [25]. This work was very broad in scope, giving potential curves for states of all symmetry types and including purely repulsive states, but at the cost of using smaller basis sets for the (many) potential curves. Their smaller basis (basis A) was used to generate the potential curves. This consisted of the chlorine basis described above [18], i.e., $5s5p2d$ + bond functions + Rydberg functions. Their larger basis B, used only for vertical excitation energies, contained $8s5p1d1f$ contracted AO's on the nuclear centers, plus (s,p) bond functions; this is similar to the basis set we used. Using basis A these authors reported potential curves for $^3\Sigma_g^-$, $^1\Delta_g$ and $^1\Sigma_g^+$ states which contain deep minima, as well as shallow minima for a number of other states. They do not report the effective well depth for these states, but we estimate from their published potential curves (see also Ref. [26]) that the well depths are 2.1, 1.2, and 0.8 eV for the three states. This is close to our own results, except that their $^3\Sigma_g^-$ state is more deeply bound (by 0.4 eV).

Another measure of the accuracy of the calculated potential curves is comparison with the observed vibrational transitions in the $^3\Sigma_g^-$ manifold. McConkey *et al.* [26] report vibrational transitions between adjacent levels over the range $v = 0 - 4$ to be approximately 80 meV. Our own calculation of the bound states for the transitions $0 \rightarrow 1$, $1 \rightarrow 2$, etc., gave 77.6, 78.1, 78.6, and 78.4 meV (see above), in excellent agreement with their experimental data.

Obviously the three bound states in Cl_2^{2+} show a significant deviation from purely Coulombic behavior. This deviation is plotted in the inset to Fig. 1 for the $^3\Sigma_g^-$ (solid line) and $^1\Delta_g$ (dashed line) states. For this plot the Coulomb potential was obtained by equating the total energy at 20 bohr (noninteraction region) to the MRD-CI value, where $E_{20} = -918.30679$ hartree, so that $E_\infty = E_{20} - (+1)(+1)/20 = -918.35679$ hartree, and then using $E_R = E_\infty + 1/R$. In each case the maximum deviation occurs near 3.38 bohr, which is slightly inside the value for $R_e(3.56, 3.62$ bohr). The deviation from Coulombic behavior is substantial, reaching a maximum value of 4.83 eV for $^3\Sigma_g^-$ (at $R = 3.41$ bohr), and 4.14 eV for $^1\Sigma_g^+$ (at $R = 3.36$ bohr).

Cl_2^{3+}. Very recently the TOF mass spectrum of the three halogen trications Cl_2^{3+}, Br_2^{3+}, and I_2^{3+} by some of the present authors has proven that all three are metastable [8]. In the latter work we gave a theoretical treatment of Cl_2^{3+} using an MRD-CI method [21–23] similar to that in the
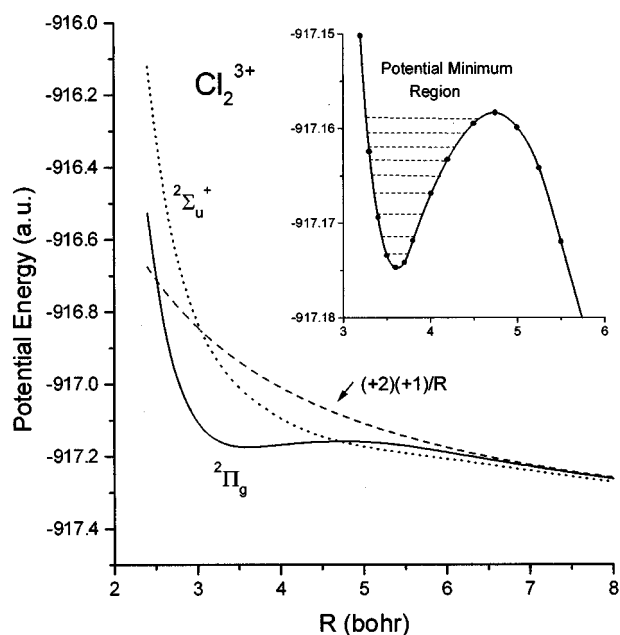
FIG. 2. Potential curves for Cl_2^{3+}, showing metastable minimum for the ground state $^2\Pi_g$. Dashed line: Coulomb potential. Inset: Expanded view of the potential minimum region, showing bound vibrational states.

present paper and reported a metastable minimum for Cl_2^{3+} [8]; other recent work also discussed the metastability of I_2^{3+} [33,9]. There are few such examples of metastable diatomic trications, although a very recent one is the observation of TiF^{3+} [34]. Here we give more details on the Cl_2^{3+} system.

SCF-MO's were generated using the triplet configuration for Cl_2^{2+}. The ground electronic state of the trication has MO occupation ...$(2\pi_g)^1$ and state symmetry $^2\Pi_g$ (Table I), corresponding to a nominal bond order of 2.5. Another MO configuration with the same bond order corresponds to the excitation $2\pi_g \rightarrow 5\sigma_u$, i.e., the excitation from one antibonding orbital to another (higher-lying). The resulting $^2\Sigma_u^+$ state may also contain a potential minimum.

Figure 2 shows the potential curves for Cl_2^{3+} along with the Coulomb potential for Cl^{2+} interacting with Cl^+. The Coulomb potential was obtained as in the dication by pinning the Coulomb curve to the MRD-CI value at 20 bohr. In this case the Coulomb potential arises from the repulsion between $+2$ and $+1$ ions and has the form $E_R = E_\infty + 2/R$, where $E_\infty = -917.50879$ hartree. The properties derived from the metastable ground state are given in Table IV.

There is clearly a metastable state formed for $^2\Pi_g$, although not for $^2\Sigma_u^+$; in fact, we found no other doublet

TABLE IV. Properties of the potential curve for Cl_2^{3+} in its lowest-lying $^2\Pi_g$ electronic state.

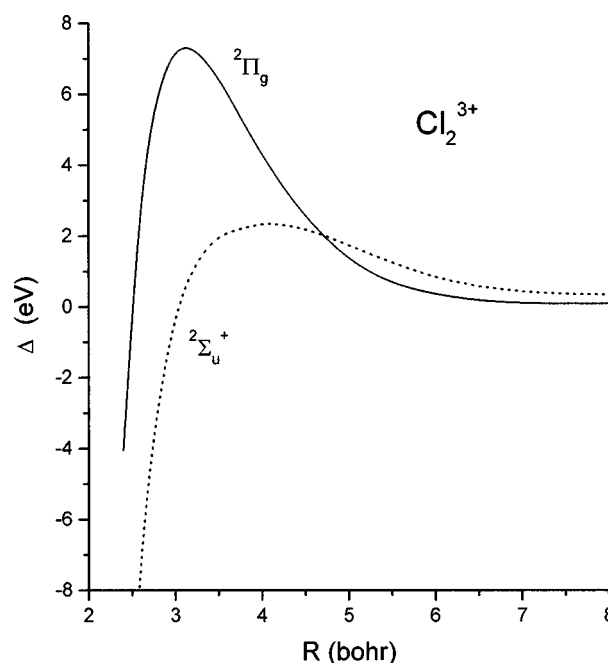|	
R_e (bohr)	3.622
R_{max} (bohr)	4.731
D_{eff} (eV)	0.447
ZPE (eV)	0.033
ω_{01} (cm^{-1})	529
No. v levels	9

FIG. 3. Deviation from Coulomb potential for the two lowest-lying states of Cl_2^{3+}.

states which were metastable. At $R = 3.60$ bohr (near the potential minimum) the CI wave function is dominated by the ground state configuration ...π_g^1, which is present in amount 80% (square of coefficient representing this configuration in the CI expansion $= 0.8$). Thus this strongly bonding description dominates the wave function, in spite of the $+3$ charge; this can be termed "residual chemical bonding." Near the maximum in the effective barrier at 4.8 bohr, however, there is very strong configuration mixing. At this point the $\pi_u^4 \pi_g^1$ configuration (bond order 2.5) represents only 50% of the CI wave function. An additional 20% arises from the configuration $\pi_u^2 \pi_g^3$ (bond order 1.5) and the remainder arises from more highly excited (antibonding) configurations. Thus the residual bonding effect is damped and the deviation from the Coulombic potential is reduced.

Bound vibrational states for the ground state $^2\Pi_g$ were computed as in the dication and are shown in Fig. 2 as an inset. The 0-1 transition occurs at 529 cm^{-1}, and there are 9 bound states behind the effective barrier. The height of the effective barrier (relative to the potential minimum) is 0.447 eV in the current treatment, compared to 0.288 eV in our previous work [8]. The reason for the deeper well obtained in the current treatment is due mostly to the use of a better basis set; the basis set used previously gave only ca. 70% of the well depth of the neutral Cl_2 molecule. However, the position of the minimum is close to that of the previous treatment (3.62 in the current treatment vs 3.67 bohr, previously).

The deviation from the Coulombic potential for the two electronic states is shown in Fig. 3. The maximum deviation of 7.28 eV occurs for $^2\Pi_g$ at 3.14 bohr. Compared to the dication Cl_2^{2+}, the deviation from Coulombic behavior has increased and the position of the maximum has shifted inwards. The $^2\Sigma_u^+$ state shows much smaller deviations from the Coulombic potential for $R \geqslant 3$ bohr. By $R = 6.0$ bohr both deviation curves approach zero, showing the disappearance of bonding effects at this internuclear distance.
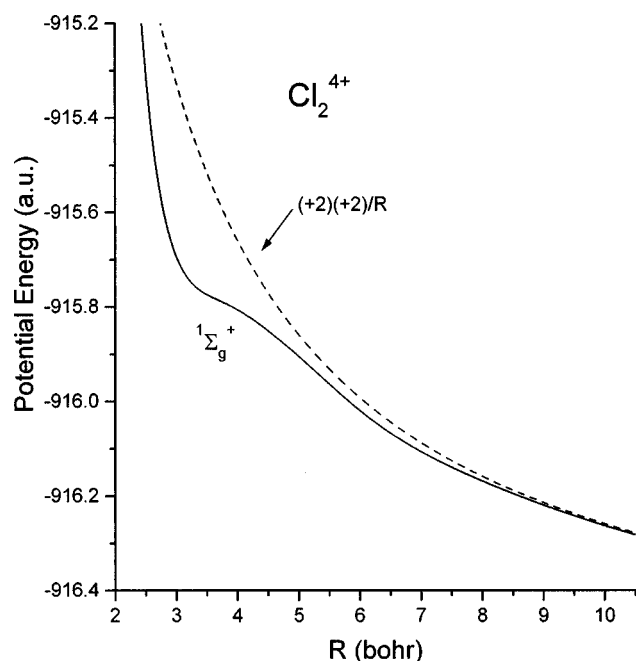
FIG. 4. Potential curve for Cl_2^{4+} in the lowest-lying electronic state. Dashed line: Coulomb potential.

FIG. 5. Potential curves for Cl_2^{6+} in the two lowest-lying electronic states. Dashed line: Coulomb potential.

Note that both potential curves show very large *negative* deviations at small R. This is a general feature of molecular potential curves—at small R, the repulsion will always be greater than the Coulombic potential characteristic of the ions formed on dissociation. The reason for this increased repulsion is that as the atomic electron clouds overlap the repulsion between the positive cores becomes increasingly unshielded, resulting in a rapidly rising potential. In Coulomb explosion experiments there is no mechanism which causes sampling of these regions of small R, so these negative deviations are not observed.

Cl_2^{4+}. The ground electronic state of the $+4$ ion has a closed-shell MO occupation with state symmetry $^1\Sigma_g^+$ and bond order 3.0, the maximum possible ground-state bond order for main-group elements built from s and p electrons in the outer (valence) shell. This ion is therefore an ideal candidate to show strong residual chemical bonding and significant deviation from a purely Coulombic potential. This can occur in spite of the high charge which causes maximum repulsion in the symmetric dissociation channel leading to $Cl^{2+} + Cl^{2+}(+4/R)$, and is still significant in the asymmetric channel $Cl^{3+} + Cl^+(+3/R)$. As with the dication there is a high-lying asymetric channel corresponding to $Cl^{4+} + Cl$ which will be attractive due to charge-induced polarization ($-2\alpha/R^4$, where α is the static dipole polarizability of Cl); mixing of this state with the other more symmetric configurations at small R may induce a metastable minimum. These excited channels lie rather far above the ground state (16 and 56 eV above the charge-symmetric channel for $+3,+1$ and $+4,+0$, respectively; see Table VI), however, which weakens the interaction. Also, it must be considered that in Cl_2^{4+} there is a much stronger asymptotic repulsion than in the trication or dication, which must be overcome by any residual bonding effect plus mixing with the attractive channel in order to create a local minimum.

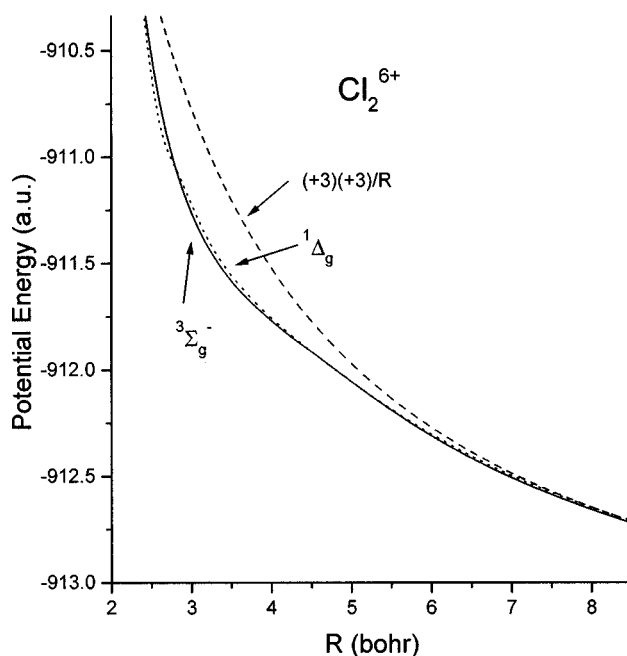SCF-MO's were generated using the ground-state singlet

MO occupation given in Table I. At 20 bohr the electronic energy is -916.45875 hartree, and the Coulomb potential is given by $E_R = E_\infty + 4/R$, where $E_\infty = -916.65875$ hartree. Figure 4 shows the potential energy curve for this state along with the Coulomb potential. There is obviously a shoulder in the potential curve showing the effects of residual bonding. At $R = 3.8$ bohr (near the vertical excitation from Cl_2) the configuration description is predominantly (73%) that of the strongly bonding $\ldots(5\sigma_g)^2(2\pi_u)^4$, with ca. 10% contribution from the excitation $\pi_u^2 \rightarrow \pi_g^2$ (less strongly bonding, B.O.$=1.0$). In other words, there is relatively little mixing with less strongly bonding excited configurations and the $+4$ ion has retained the "memory" of its strong-bonding configuration in this region. However in this case the Coulomb repulsion is too strong to be overcome and no metastable minimum is formed. The defect Δ, which now exceeds 10 eV, is shown on the composite Fig. 6.

Cl_2^{6+}. The $+6$ ion has MO occupation $\ldots(2\pi_u)^2$, leading to three low-lying states of $^3\Sigma_g^-$, $^1\Delta_g$ and $^1\Sigma_g^+$ symmetry, each with B.O.$=2.0$. Figure 5 shows the two lowest electronic states $^3\Sigma_g^-$ and $^1\Delta_g$, and the Coulomb repulsion potential for two ions of charge $+3$. The two electronic states are almost superimposed, and on the scale of the drawing the $^1\Sigma_g^+$ would be almost coincident with the other two. All three electronic states therefore show a significant deviation from the Coulomb potential. The maximum in this deviation occurs near $R = 3.0$ bohr, and in this region the CI wave function for the triplet state contains the ground-state configuration $\ldots(5\sigma_g)^2(2\pi_u)^2$ with 90% weight, i.e., essentially a single-configuration description. At $R = 4.0$ bohr the single-configuration description has only dropped to 77%, consistent with the fact that the deviation from the Coulombic potential is still substantial. At $R = 8.0$ bohr and larger, the deviation from the Coulomb potential is negligible for all three electronic states.

Cl_2^{8+}.   The $+8$ ion   has   MO   occupation
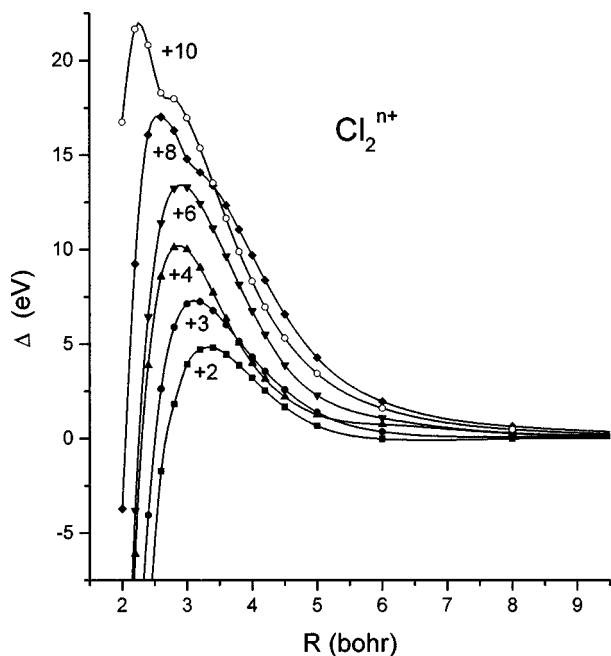
FIG. 6. Composite graph of deviations from Coulomb potential for the diatomic chlorine ions Cl_2^{n+} in their ground states.

TABLE V. Absolute and relative energies for diatomic chlorine ions at 3.8 bohr. The ΔE's in the table correspond to $Cl_2^{(n)+} \rightarrow Cl_2^{(n+1)+}$, i.e., the vertical excitation energy (excluding zero-point energy) calculated at 3.8 bohr.

Ion (state)	E_{CI}[a] (hartree)	ΔE (eV)
$Cl_2(^1\Sigma_g^+)$	-919.35648	0.000
$Cl_2^+(^2\Pi_g)$	-918.93941	11.35
$Cl_2^{2+}(^3\Sigma_g^-)$	-918.23639	19.13
$Cl_2^{3+}(^2\Pi_g)$	-917.17189	28.97
$Cl_2^{4+}(^1\Sigma_g^+)$	-915.79223	37.54
$Cl_2^{5+}(^2\Pi_u)$	-913.92091	50.92
$Cl_2^{6+}(^3\Sigma_g^-)$	-911.70183	60.38
$Cl_2^{7+}(^2\Pi_u)$	-909.06836	71.66
$Cl_2^{8+}(^1\Sigma_g^+)$	-906.06553	81.71
$Cl_2^{10+}(^1\Sigma_g^+)$	-898.70646	
$Cl_2^{12+}(^1\Sigma_g^+)$	-888.92459	

[a]Includes the Langhoff-Davidson correction [23] to the MRD-CI energy.

$\ldots (5\sigma_g)^2(2\pi_u)^0$, leading to an electronic state of $^1\Sigma_g^+$ symmetry. Another MO occupation which should be considered is $\ldots (5\sigma_g)^0(2\pi_u)^2$, particularly since the $2\pi_u$ MO is more strongly bonding than the $5\sigma_g$ [35]. Two low-lying electronic states formed from this configuration are $^3\Sigma_g^-$ and $^1\Delta_g$. The bond order is now reduced to 1.0 in both cases, i.e., little residual bonding is expected in the $+8$ ion.

SCF-MO's were generated for the triplet (π_u^2) configuration and used in all cases. The ground state over most of the range is the $^1\Sigma_g^+$ state (solid line), although both the $^3\Sigma_g^-$ and $^1\Delta_g$ states lie (slightly) lower for $R \leq 3$ bohr. The two excited electronic states (at $R \geq 3$ bohr) lie very close together. For all three states the deviations from the Coulombic potential are substantial. A maximum deviation of 17.03 eV is reached for $^1\Sigma_g^+$ at 2.61 bohr, and 19.31 eV for $^3\Sigma_g^-$, also at 2.61 bohr. A plot of Δ for the lower-lying $^1\Sigma_g^+$ state is shown in Fig. 6.

Cl_2^{10+}. The $+10$ ion has a formal bond order of zero, so no residual bonding is expected. There may still be deviations from the Coulomb potential, however, e.g., along the inner wall of the potential. For this ion the SCF-MO's were generated from the closed-shell configuration given in Table I. Inspection of the Coulomb deviation in Fig. 6, however, shows that there is still significant deviation even for the case where the bond order is formally zero.

IV. DISCUSSION

A. Vertical ionization potentials/excitation energies

The calculated equilibrium internuclear distance for neutral diatomic chlorine $(Cl_2, X^1\Sigma_g^+)$ is $R_e = 3.820$ bohr (expt. 3.757 bohr, Table II). Since data values were taken at 3.8 bohr, this value of R was used to obtain an estimate of the vertical excitation energies to create the various charged ions. (More rigorous treatment would require correction for

zero-point energies, but in the bound molecules including neutral Cl_2 these corrections do not exceed 0.04 eV). Table V gives the MRD-CI energy for each ion up to Cl_2^{12+} in its ground electronic state, including the ions Cl_2^{5+} and Cl_2^{7+}, along with the stepwise excitation energy.

For the first two ionizations these data can be compared to the theoretical vertical excitation values of Fournier *et al.* [25] and to the experimental appearance potentials. Using their larger basis B Fournier *et al.* obtained 11.36 eV and 19.25 eV for IP$_1$ and IP$_2$, respectively. These are close to our own values in Table V but below the experimental appearance potentials [26], which appear for the dication at IP$_1$ + IP$_2$ = 31.13 eV by 0.52 eV [25] or 0.65 eV (our calculation). Note, however, that because of the significant shift in R_e it is possible that a ''hot band'' may have been observed in the experiment, which would serve to increase the appearance potential.

From Table V a useful generalization emerges: there is an increment of 10 ± 2 eV on successive ionizations, i.e., the first ionization requires approximately 10 eV, the second requires 20 eV, etc. This trend would only be expected to continue as long as valence electrons from the $3p$-manifold are being removed; two such electrons remain in Cl_2^{8+}, which has a total of 6 remaining valence electrons. Therefore the next two ionizations forming Cl_2^{9+} and Cl_2^{10+} should require ca. 90 and 100 eV, respectively. To check this the energy of Cl_2^{10+} was found to be 200 eV above the energy of Cl_2^{8+}, close to the simple prediction of 190 eV. Beyond Cl_2^{10+} there will be a jump in ionization energy since the next four electrons are being removed from MO's built predominantly from $3s$ AO's. Thus the energy of Cl_2^{12+} was calculated to lie 266 eV above the energy of Cl_2^{10+} (Table V). Still further ionization beyond Cl_2^{14+} will enter a very-high energy regime where inner-shell electrons are being removed.

B. Symmetric and asymmetric dissociation channels

One of the features of high-energy Coulomb explosions is the possibility of multiple dissociation channels, e.g., both

TABLE VI. Relative experimental energies of the symmetric and asymmetric dissociation channels for the even-charged diatomic chlorine ions.

Species	Ion channel	E_{rel} (eV)
Cl_2^{2+}	$+1, +1$	0.000
	$+2, 0$	10.846
Cl_2^{4+}	$+2, +2$	0.000
	$+3, +1$	15.796
	$+4, 0$	56.294
Cl_2^{6+}	$+3, +3$	0.000
	$+4, +2$	13.855
	$+5, +1$	57.841
	$+6, 0$	141.904
Cl_2^{8+}	$+4, +4$	0.000
	$+5, +3$	14.335
	$+6, +2$	71.755
	$+7, +1$	162.137
	$+8, 0$	497.449

symmetric and asymmetric channels. For example, Cl_2^{8+} can dissociate into the symmetric channel $(4+, 4+)$ or the asymmetric channels $(5+, 3+), (6+, 2+)$, etc. and one of the observables in these experiments is the ratio of the ions produced in each channel [36,1]. The energies of the various dissociative channels from tabulated values for the experimental ionization potentials [37] are given below in Table VI. These ion channel energies correspond to the dissociated ions in their ground electronic states. Thus Cl_2^{2+} dissociates into $2Cl^+$ ions; since this is the lowest energetic state for the dication (which is metastable) it is assigned a relative value of 0.00. The channel corresponding to $Cl + Cl^{2+}$ lies 10.846 eV above $2Cl^+$, etc.

In every case, the symmetric channel is energetically the lowest-lying. The first excited channel for the four cases lies only 11–16 eV above the symmetric channel which is low enough in energy to allow mixing into the CI wave function, when permitted by spin and symmetry selection rules. Energies of the more asymmetric channels rise rapidly.

C. Deviation from Coulomb potential and residual chemical bonding

A composite graph for the deviation from a Coulombic potential is shown in Fig. 6, for the ions $+2, +3, +4, +6,$ $+8$ and $+10$. The most striking observation is that the Coulomb deviations are huge, reaching over 20 eV in the case of the $+10$ ion. This is even more remarkable when one considers that the formal bond order for the $+10$ ion is zero, so no deviation at all was expected. A second observation is that there is a general inward shift in the position of the maximum in Δ. These observations are the most important results in this work, and we inquire here into their physical origin.

The corresponding bond order for the ground-state configuration is 2.0, 2.5, 3.0, 2.0, 1.0, and 0.0, respectively. On that basis alone, the deviation Δ should increase on going from Cl_2^{2+} (B.O. $= 2.0$) to Cl_2^{4+} (maximum B.O. $= 3.0$) and then begin to decrease, reaching zero for the ion Cl_2^{10+}. Furthermore, since the bond distance is inversely related to

the bond order, the equilibrium internuclear distance R_e should shift inwards as the charge increases, provided that a single-configuration description of the CI wave function is a reasonable representation near the potential minimum. This would be expected to cause an inward shift in the position of the maximum in Δ with increasing bond order, and a subsequent outward shift as the bond order is reduced in the more highly charged ions.

Figure 6 shows that there is some validity to these simple predictors, as well as some surprises. First, consider the asympotic properties of Δ. As explained earlier, at small R the value of Δ will be negative due to penetration of the ion cores and the consequent increased repulsion. At large R, Δ will approach zero (true for all potential curves and obvious in Fig. 6) as the interaction resembles point charges at large internuclear distance. At intermediate R the deviation Δ will go through a maximum provided that the molecular ion retains residual chemical bonding. The general shape of $\Delta(R)$ is therefore known in advance of calculation.

Second, consider the position of the maximum in Δ along the internuclear coordinate, as a function of ion charge. The deviation Δ will continue to increase as long as the slope of the Coulomb potential is larger than that of the true potential curve. Since the slope of the true potential is minimal (or zero) near R_e and remains smaller than the Coulomb curve for some range of $R < R_e$, this causes Δ to maximize at $R < R_e$.

A simple physical model which shows these general features is the following: A single electron is placed midway between two like charges $+Q$ separated by a distance R. The electrostatic energy is then $V = (Q^2 - 4Q)/R$. The kinetic energy is approximated by a particle in a 3D box whose dimension is $(R - a)$, where a is an adjustable constant which allows for the fact that the box length is somewhat smaller than R. The kinetic energy is then $T = 3h^2/8ml^2$, where $l = R - a$, and m is the electron mass. In atomic units $T = 3(2\pi)^2/8(R - a)^2$. The difference between the Coulomb potential Q^2/R and the molecular potential $T + V$ is then given by $\Delta = const[4Q/r - 3(2\pi)^2/8(R - a)^2]$, where const is a scale factor to bring the axis into correspondance with Fig. 6. Using $a = 1$ bohr and const $= 0.25$ for all the diatomic ions, Fig. 7 shows the plot of $\Delta(R)$ vs R for the ions of charge $+2$ through $+10$. The attenuation of Δ with R is much slower than that shown in Fig. 6 for the true systems, but the general behavior is correct: There is an approximately linear increase in Δ with Q, and there is an inward shift in the position of the maximum with increasing Q.

A third, and much smaller effect, is the shift in the value of R_e as the bond order increases on ionization from neutral Cl_2. There is a small inward shift in R_e on ionization from neutral Cl_2, going from 3.82 bohr in Cl_2 (calculated value, Table II) to 3.64 bohr in Cl_2^+ to 3.57 bohr in Cl_2^{2+} (Table III). This is consistent with the increasing bond order (1.0, 1.5, 2.0, respectively). However, the position of the minimum shifts outward again in Cl_2^{3+} to 3.62 bohr, in spite of the fact that the bond order has further increased to 2.5. In order to understand these results, it is necessary to consider the composition of the CI wave function, which is changing with internuclear distance, as well as the asympotic behavior of the Coulomb deviation.
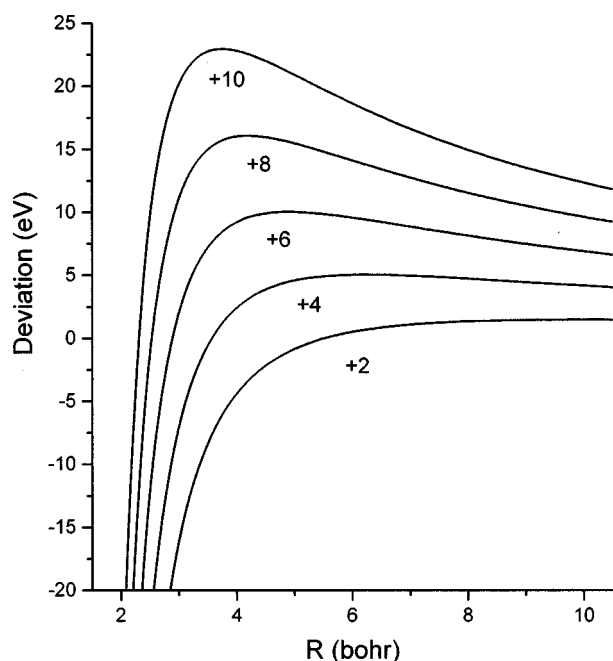
FIG. 7. Deviation of simple model from Coulomb potential for diatomic ions with total charge $+n$, where $n = 2Q$.

In the case of Cl_2^{2+}, below $R = 3.0$ the wave function contains $\geqslant 90\%$ of the ground-state configuration $\dots \pi_g^2$ (bond order $= 2.0$). At $R = 4.0$ the composition has dropped to 83% of Ψ_1, the maximally bonding configuration, and contains 4% of the configuration corresponding to the double excitation $\pi_u^2 \rightarrow \pi_g^2$ (zero bond order). At 5.0 bohr which is near the potential maximum the contribution of Ψ_1 has dropped to 61% and additional excitations of the form $\sigma_g^2 \rightarrow \sigma_u^2$ enter strongly (bond order zero). Here the total wave function becomes roughly an equal mixture of bonding and nonbonding configurations, necessary to allow dissociation into $Cl^+ + Cl^+$. Finally, at large R the contribution of Ψ_1 approaches zero.

The general result is that the position of the minimum in the potential curve will only continue to move inward as bond order increases, so long as a pure (maximum bonding) single-configuration description remains valid. For Cl_2^{4+} for example, in its ground state $^1\Sigma_g^+$, at $R = 4.0$ bohr the strongly bonding configuration $\dots \sigma_g^2 \pi_u^4$ is only 63% of the CI wave function, and the double excitations $\pi_u^2 \rightarrow \pi_g^2$ already make important contributions. When this situation holds, the bond order is less than the nominal value predicted from simple MO theory, and the position of the minimum in the potential curve will shift to larger R. This is the situation which is observed in comparing Cl_2^{3+} to Cl_2^{2+}: the decline of the single-configuration description begins earlier (in R) for the more highly charged ion.

Finally, consider why there appears to be residual chemical bonding for Cl_2^{10+}, an ion which has zero formal bond order. Analysis of the CI wave function for Cl_2^{10+} shows that at $R = 3.8$ bohr, the (nonbonding) configuration $\dots 4\sigma_g^2 4\sigma_u^2$ does indeed contribute 94% to the total. Moving inwards, at $R = 2.80$ bohr, where a shoulder on the plot of Δ appears (Fig. 6), the wave function consists of 88% of $\sigma_g^2 \sigma_u^2$; however, it also contains 4% of the (excited) strongly

bonding configuration $\sigma_g^2 \pi_u^2$ and 4% of another bonding configuration $4\sigma_g^2 5\sigma_g^2$. At $R = 2.20$ bohr, which is near the maximum in Δ vs R, the wave function consists of 0% of the nonbonding $\sigma_g^2 \sigma_u^2$ but 96% of the bonding configuration $\sigma_g^2 \pi_u^2$. The ion Cl_2^{10+} therefore maintains residual bonding at small R, and indeed shows its maximum in Δ at $R = 2.26$ bohr, exactly the region in which an unexpected bonding configuration is dominant.

The apppearance of strongly bonding configurations at small internuclear distances is exactly what would be predicted from the avoided crossing model. In Cl_2^{2+}, for example, the asymetric channel correlating with $Cl + Cl^{2+}$ lies 11 eV above the repulsive channel $Cl^+ + Cl^+$. The charge-induced polarization as asymmetric $Cl + Cl^{2+}$ approach is attractive, and this diabatic potential curve shows an avoided crossing with the repulsive potential curve correlating with the symmetric ions $Cl^+ + Cl^+$. A minimum therefore results at small R. When the charge becomes higher the asymptotes also lie higher in energy, so the effects persist but manifest themselves at even smaller internuclear distances. This causes a deviation from the Coulomb potential, which is observed in Fig. 6.

V. SUMMARY AND CONCLUSIONS

Using the MRD-CI approach described in this paper, good results have been obtained for potential curves in two cases where the experimental data were known, namely Cl_2 and Cl_2^+. The calculations were extended by the same methods to give potential energy curves out to dissociation for the ions Cl_2^{2+}, Cl_2^{3+}, Cl_2^{4+}, Cl_2^{6+}, Cl_2^{8+} and Cl_2^{10+}. In each case, sufficient reference configurations were used in the CI expansion so that the reference configurations contributed $\geqslant 90\%$ to the final CI expansion; this ensured smooth behavior of the potential curve out to dissociation.

The Cl_2^{2+} dication has at least three bound metastable states, the most deeply bound of which is $^3\Sigma_g^-$. Calculation of the vibrational spectrum for this state shows good agreement with the measured vibrational spacing [26]. The $^3\Sigma_g^-$ state shows a deviation from the Coulomb potential of almost 5 eV, and at a distance which is close to that arising from vertical excitation from Cl_2. The Cl_2^{3+} ion is metastable in its ground electronic state $^2\Pi_g$, with an effective potential well of 0.45 eV. This is in agreement with the reported metastability by experimental measurement [8]. The Cl_2^{4+} ion has the largest bond order in the series (3.0) and shows a pronounced shoulder relative to the Coulomb potential. The remaining ions Cl_2^{6+}, Cl_2^{8+}, and Cl_2^{10+} all show substantial deviations from the corresponding Coulomb potentials, with an approximately linear increase with Q, even though the formal bond order in Cl_2^{10+} is zero. Analysis of this unexpected result for the $+10$ ion showed that it results from the dominance in the CI wave function at small R of strongly bonding excited configurations which remove the electrons from antibonding orbitals and effectively increase the bond order.

As measured by the deviation Δ from the Coulomb potential, all the ions in this study for $+2$ to $+10$ show substantial residual bonding. The use of a simple physical model

of an electron midway between two charges $+Q$ and a particle-in-a-box model for the electron kinetic energy helps to explain trends in Δ as a function of R and Q. The extent of the deviation Δ can become very large at small R, with a maximum value greater than 20 eV for the $+10$ ion. In the region of vertical excitation (near $R = 3.80$ bohr) the value of Δ is near 5 eV for the ions Cl_2^{2+}, Cl_2^{3+}, Cl_2^{4+}, and closer to 10 eV for Cl_2^{6+}, Cl_2^{8+}, and Cl_2^{10+}.

These data can now be used to help in the interpretation of Coulomb explosion experiments, and to try to give a complete mechanism for dissociation through a manifold of ion states in MEDI experiments on diatomic chlorine. What remains to be done is to consider the modification of the potential energy curves for the various ions in an intense laser field. This occurs by interaction with the molecular polarizability, which can increase the kinetic energy defect, and will be discussed in a later publication.

ACKNOWLEDGMENTS

[1] E.P. Kanter, P.J. Cooney, D.S. Gemmell, K.-O. Groeneveld, W.J. Pietsch, A.J. Ratkowski, Z. Vager, and B.J. Zabransky, Phys. Rev. A **20**, 834 (1979).

[2] Z. Vager, R. Naaman, and E.P. Kanter, Science **244**, 426 (1989); J. Levin, H. Feldman, A. Baer, D. Ben-Hamu, O. Heber, D. Zajfmen, and Z. Bager, Phys. Rev. Lett. **81**, 3347 (1998).

[3] M. Nisoli *et al.*, Opt. Lett. **22**, 522 (1997).

[4] H. Stapelfeldt, E. Constant, and P.B. Corkum, Phys. Rev. Lett. **74**, 3780 (1995); C. Ellert, H. Stapelfeldt, E. Constant, H. Sakai, J.S. Wright, D.M. Rayner, and P.B. Corkum, Philos. Trans. R. Soc. London, Ser. A **356**, 329 (1998).

[5] D. Mathur, K. Krishnakumar, K. Nagesha, V.R. Marathe, V. Krishnamurthi, and V.T. Raheja, J. Phys. B **26**, L141 (1993).

[6] C. Cornaggia, C. Normand, and J. Morellec, J. Phys. B **25**, L415 (1992).

[7] H. Sakai, H. Stapelfeldt, E. Constant, M.Yu. Ivanov, D.R. Matusek, J.S. Wright, and P.B. Corkum, Phys. Rev. Lett. **81**, 2217 (1998).

[8] P.J. Bruna and J.S. Wright, J. Phys. B **26**, 1819 (1993).

[9] G. Handke, F. Tarantelli, and L.S. Cederbaum, Phys. Rev. Lett. **76**, 896 (1996).

[10] M. Schmidt, D. Normand, and C. Cornaggia, Phys. Rev. A **50**, 5037 (1994).

[11] M. Brewczyk, K. Rzazewski, and C.W. Clark, Phys. Rev. Lett. **78**, 191 (1997).

[12] T. Seideman, M.Yu. Ivanov, and P.B. Corkum, Phys. Rev. Lett. **75**, 2819 (1995).

[13] K.P. Huber and G. Herzberg, *Molecular Spectra and Molecular Structure. IV. Constants of Diatomic Molecules* (Van Nostrand, Princeton, NJ, 1979).

[14] A.K. Hays, Opt. Commun. **28**, 209 (1979).

[15] M.C. Castex, J. leCalvé, D. Haaks, B. Jordan, and G. Zimmerer, Chem. Phys. Lett. **70**, 106 (1980).

[16] J.W. Cooley, Math. Comput. **15**, 363 (1961).

[17] W.J. Hehre, L. Radom, R.v.R. Schleyer, and J.A. Pople, *Ab Initio Molecular Orbital Theory* (Wiley, New York, 1986).

[18] S.D. Peyerimhoff and R.J. Buenker, Chem. Phys. **57**, 279 (1981).

[19] A.D. McLean and G.S. Chandler, J. Chem. Phys. **72**, 5639 (1980).

[20] A listing of the basis set used is available as supporting documentation for this article.

[21] R.J. Buenker, S.D. Peyerimhoff, and W. Butscher, Mol. Phys. **35**, 771 (1978).

[22] R.J. Buenker and R.A. Phillips, J. Mol. Struct.: THEOCHEM **123**, 291 (1985).

[23] S.R. Langhoff and E.R. Davidson, Int. J. Quantum Chem. **7**, 999 (1973).

[24] J.H. Beynon, R.M. Caprioli, and J.W. Richardson, J. Am. Chem. Soc. **93**, 1852 (1971).

[25] P.G. Fournier, J. Fournier, F. Salama, D. Stärk, S.D. Peyerimhoff, and J.H.D. Eland, Phys. Rev. A **34**, 1657 (1986).

[26] A.G. McConkey, G. Dawber, L. Avaldi, M.A. MacDonald, G.C. King, and R.I. Hall, J. Phys. B **27**, 271 (1994).

[27] J. Senekowitsch and S. ONeil, J. Chem. Phys. **95**, 1847 (1991).

[28] J. Senekowitsch, S. ONeil, and W. Meyer, Theor. Chim. Acta **84**, 85 (1992).

[29] D.R. Bates and T.R. Carson, Proc. R. Soc. London, Ser. A **68**, 1199 (1955).

[30] P.M.W. Gill and L. Radom, Chem. Phys. Lett. **136**, 94 (1987).

[31] M. Kolbuszewski and J.S. Wright, Can. J. Chem. **71**, 1562 (1993).

[32] The MRD-CI program works with the largest Abelian subgroup of the true point group, which in the case of $D_{\infty h}$ is D_{2h}. Both Σ_g^+ and Δ_g electronic states transform according to the A_{1g} irreducible representation of D_{2h}. The correct assignment (Σ_g^+ or Δ_g) state is made by inspection of the eigenvectors of the CI diagonalization.

[33] C. Ellert, H. Stapelfeldt, E. Constant, H. Sakai, J.S. Wright, D.M. Rayner, and P.B. Corkum, Philos. Trans. R. Soc. London, Ser. A **356**, 329 (1998).

[34] D. Schröder, J.N. Harvey, and H. Schwarz, J. Phys. Chem. A **102**, 3639 (1998).

[35] P.J. Bruna and J.S. Wright, J. Chem. Phys. **91**, 1126 (1989).

[36] D.T. Strickland, Y. Beaudoin, P. Dietrich, and P.B. Corkum, Phys. Rev. Lett. **68**, 2755 (1992).

[37] *CRC Handbook of Chemistry and Physics, 75th Edition*, edited by D.R. Lide (CRC Press, Boca Raton, 1995).